water

MDPI

Article

Influence of Water Salinity on the Efficiency of Fe^0-Based Systems for Water Treatment

Ran Tao [1], Xuesong Cui [1], Minhui Xiao [1,2], Rui Hu [2], Willis Gwenzi [3,4], Hans Ruppert [5] and Chicgoua Noubactep [1,6,7,8,*]

1 Applied Geology, University of Göttingen, Goldschmidtstraße 3, D-37077 Göttingen, Germany; ran.tao@stud.uni-goettingen.de (R.T.); cuixuesonghhu17@163.com (X.C.); xiaominhui@hhu.edu.cn (M.X.)
2 School of Earth Science and Engineering, Hohai University, Fo Cheng Xi Road 8, Nanjing 211100, China; rhu@hhu.edu.cn
3 Grassland Science and Renewable Plant Resources, Faculty of Organic Agricultural Science, University of Kassel, Steinstrasse 19, D-37213 Witzenhausen, Germany; wgwenzi@yahoo.co.uk
4 Leibniz Institute for Agricultural Engineering and Bioeconomy (ATB), Max-Eyth-Alle 100, D-14469 Potsdam, Germany
5 Department of Sedimentology & Environmental Geology, University of Göttingen, Goldschmidtstraße 3, D-37077 Göttingen, Germany; hrupper@gwdg.de
6 Department of Water and Environmental Science and Engineering, Nelson Mandela African Institution of Science and Technology, Arusha P.O. Box 447, Tanzania
7 Faculty of Science and Technology, Campus of Banekane, Université des Montagnes, Bangangté P.O. Box 208, Cameroon
8 Centre for Modern Indian Studies (CeMIS), Universität of Göttingen, Waldweg 26, D-37073 Göttingen, Germany
* Correspondence: cnoubac@gwdg.de

Abstract: Metallic iron (Fe^0) is a reactive material for treating polluted water. The effect of water salinity on the efficiency of Fe^0-based remediation systems is not yet established. This work aims to clarify the reasons why Cl^- ions are often reported to improve the efficiency of Fe^0/H_2O remediation systems. Quiescent batch experiments were carried out to characterize the effect of chloride (Cl^-) ions on the efficiency of methylene blue (MB) discoloration in the presence of Fe^0. Cl^- was used in the form of NaCl at concentrations ranging from 0 to 40 g L^{-1}. The MB concentration was 10 mg L^{-1}, the Fe^0 loading was 5 g L^{-1}, and the duration of the experiment varied from 2 to 46 days. Four different Fe^0 materials were tested in parallel experiments. Tests with different NaCl levels were performed in parallel with three other organic dyes: Methyl orange (MO), orange II (OII), and reactive red 120 (RR 120). The results clearly show that the presence of Cl^- reduces the extent of dye discoloration in all systems investigated. The efficiency of the dyes increased in the order MB < MO < RR 120 < OII. In systems with varying NaCl concentrations, dye discoloration initially decreases with increasing NaCl and slightly increases for [NaCl] > 30 g L^{-1}. However, the extent of dye discoloration for [NaCl] = 40 g L^{-1} remains much lower than for the system with [NaCl] = 0 g L^{-1}. The results clearly demonstrate that the presence of Cl^- fundamentally delays the process of contaminant removal in Fe^0/H_2O systems, thus improving the understanding of the contaminant interactions in Fe^0-based remediation systems. These results also suggest that the effects of other inorganic anions on the efficiency of Fe^0/H_2O systems should be revisited for the design of field applications.

Keywords: chloride ions; groundwater remediation; permeable reactive barriers; water salinity; zero-valent iron

check for updates

Citation: Tao, R.; Cui, X.; Xiao, M.; Hu, R.; Gwenzi, W.; Ruppert, H.; Noubactep, C. Influence of Water Salinity on the Efficiency of Fe^0-Based Systems for Water Treatment. *Water* **2023**, *15*, 2466. https://doi.org/10.3390/w15132466

Academic Editors: Alexandre T. Paulino and Andreas Angelakis

Received: 2 June 2023
Revised: 26 June 2023
Accepted: 3 July 2023
Published: 5 July 2023

Copyright: © 2023 by the authors. Licensee MDPI, Basel, Switzerland. This article is an open access article distributed under the terms and conditions of the Creative Commons Attribution (CC BY) license (https://creativecommons.org/licenses/by/4.0/).

1. Introduction

Population growth and climate change are causing freshwater resources to decline worldwide [1,2]. The situation is exacerbated in coastal regions where seawater intrusion occurs as a result of unsustainable water management strategies [3,4]. In cities, poor

planning and weather forecasting also contribute to sewage pollution [5,6]. To address the issue of water scarcity, preventing water pollution and treating and reusing wastewater are becoming increasingly important everywhere [5,6]. In this context, the need for affordable, applicable, but efficient technology cannot be overemphasized, particularly for low-income communities [7,8]. The use of metallic iron (Fe^0) in water treatment systems is one such an affordable technology that has been shown to be highly efficient for decentralized and safe drinking water supplies [7] and wastewater treatment [8]. However, the effect of water salinity on the efficiency of Fe^0/H_2O remediation systems has not yet been adequately addressed [9,10].

Metallic iron (Fe^0), as a reactive material, has been tested and used extensively within the water treatment industry over the last three decades [11–23]. The discovery of Fe^0-based permeable reactive barriers (Fe^0 PRBs) in the early 1990s was the starting point for intensive research, the results of which have been documented in several thousand scientific publications [16,24–27]. However, despite these efforts, the fundamental mechanistic understanding of the processes controlling the efficiency of Fe^0-based remediation systems is not well-established [21,28–32]. In other words, there is still no scientific consensus on how to design a sustainable Fe^0 PRB [21,28,30–34].

Despite conflicting reports in the literature, all researchers would agree with the following statement by Matheson and Tratnyek [35], describing the importance of mechanistic understanding in system design: "The effective design and operation of these systems will be improved by a more detailed process-level understanding of iron/contaminant interactions in porous media". The results of these authors suggest that Fe^0 exchanges electrons with dissolved contaminants or that contaminant reduction is a cathodic reaction coupled with the simultaneous oxidative dissolution of Fe^0 (anodic reaction). Several research groups did not confirm these findings [36–41]. The most prominent example is certainly Jiao et al. [40] who, using the same species (e.g., CCl_4), elegantly demonstrate that Fe^0 plays no role in the process of CCl_4 reductive transformation in the Fe^0/H_2O system. Later, Ebelle et al. [42] showed that the experimental conditions of Matheson and Tratnyek [35] were not suitable for them to draw their main conclusions. A number of papers have shown that the view that Fe^0 is a reducing agent is based on results from inappropriate experimental conditions [13,17,30,33,43–45]. For example, experimental conditions (e.g., shaking, stirring) that prevent the diffusive transport of contaminants near the Fe^0 surface give reproducible results in the laboratory but are not relevant for Fe^0 PRBs in the field [13,18,28,30,45–49].

Apparently, none of the arguments presented over the past 15 years have convinced the majority of active researchers to question their approach and argumentation [21,31,32,48,49]. One promising approach is the so-called MB method, which characterizes the extent of Fe^0 corrosion by monitoring the extent of methylene blue (MB) discoloration in a Fe^0/sand/H_2O system [50–54]. MB discoloration cannot be attributed to any redox reactivity within the Fe^0/sand/H_2O system but results from (i) adsorption on sand and (ii) co-precipitation with in situ generated iron corrosion products (FeCPs) [50,55]. In other words, by varying (i) the amounts of Fe^0 and/or sand or (ii) the type of Fe^0 in a Fe^0/sand/H_2O system, a number of parameters can be investigated, as MB discoloration correlates well with the extent of Fe^0 oxidation and/or the extent of generation of free FeCPs for (i) MB co-precipitation or (ii) sand surface coating. The sand surface coated with FeCPs is not a good adsorbent for MB [50,52–55]. The MB method is used here to characterize the effects of salinity (NaCl) on the efficiency of the Fe^0/H_2O system.

Several studies have investigated the effects of solution chemistry on the performance of Fe^0/H_2O systems [9,10,56–62]. In the words of Sun et al. [63], understanding such effects "will provide opportunities to assess the feasibility of this technology and to adapt the engineering design to site-specific conditions". However, with the exception of chloride, no general conclusions can be drawn because the systems investigated were limited to specific contaminants or groups of contaminants [10,63]. For chlorides, an enhancing effect on decontamination in Fe^0/H_2O systems has generally been reported [56,59,60,63,64]. This

suggests that Fe^0/H_2O systems would work well in natural saline waters containing up to 40 g/L NaCl (e.g., fracturing wastewater, groundwater, industrial wastewater, reverse osmosis concentrates) [29,65–67]. This conclusion contradicts the evidence that contaminants are removed from the aqueous solution by iron oxidhydroxides (iron corrosion products—FeCPs). In fact, when Fe^0 is dissolved by water (Equation (1)), the generated Fe^{2+} and Fe^{3+} ions primarily form relatively soluble chlorocomplexes salts (e.g., $FeCl_2$, $FeCl_3$) or low soluble oxidhydroxides, such as $Fe(OH)_2$, $Fe(OH)_3$ (Equation (2)—not stoichiometric) [48,49,68,69]. Equation (1) shows that Fe^0 corrosion consumes H^+ (or produces OH^-) and thus increases the pH of the system. Increasing the pH value favors the precipitation of Fe hydroxides (Equation (2)).

$$Fe^0 + 2\,H^+ \Rightarrow Fe^{2+} + H_2 \quad (1)$$

$$Fe^{2+} \text{ and } Fe^{3+} \Rightarrow \text{Fe salts + Fe hydroxides} \quad (2)$$

Equations (1) and (2) suggest that, if used Fe^0 produces dissolved Fe^{2+} and Fe^{3+} ions in stoichiometric abundance relative to available Cl^-, hydroxides will begin to form as Cl^- is depleted (Equation (2)). Clearly, contaminant removal in Fe^0/H_2O systems should be delayed in the presence of Cl^- (working hypothesis). This is the opposite of what has typically been reported over the years [59,60,63,64]. Therefore, the reasons for Cl^--enhanced decontamination in Fe^0/H_2O systems remain to be elucidated.

This research characterizes the effects of chloride ions on MB discoloration in Fe^0/H_2O systems by testing the validity of the working hypothesis ("the presence of Cl^- delays contaminant removal in Fe^0/H_2O systems"). Accompanying experiments are carried out with three other organic dyes (methyl orange, orange II, and reactive red 120). The results will be discussed comparatively. This research will provide more information for the actual application of Fe^0/H_2O systems. It is expected that the research will provide more information for the actual application of Fe^0/H_2O systems for saltwater remediation.

2. Material and Methods

2.1. Solutions

2.1.1. Dye Solutions

The used reagents methylene blue (MB—Basic Blue 9 from Merck, Darmstadt, Germany), methyl orange (MO—from Merck, Darmstadt, Germany), reactive red 120 (RR 120—from SIGMA company, Taufkirchen, Germany), and orange II (OII—from ACROS Organics, Geel, Belgium) were all of analytical grade. The physico-chemical characteristics of the four dyes are summarized in Table 1. The working solution for each dye was 10 mg L^{-1}. The MB solutions were prepared by diluting a stock solution of 1000 mg L^{-1}. The other three dye solutions were prepared by dissolving accurately weighed corresponding materials in tap water. Table salt from a local supermarket of Kaufland, Germany was used as the NaCl source. Weighed table salt was dissolved in tap water to prepare the working solutions. The Cl^- concentration of the tap water was considered as part of the background electrolyte (operational reference). The average composition of this water is (mg L^{-1}): Cl^-: 9.7; $NO_3{}^-$: 7.7; $SO_4{}^{2-}$: 30.0; $HCO_3{}^-$: 88.5; Na^+: 6.0; K^+: 0.5; Mg^{2+}: 7.3; Ca^{2+}: 32.6, and its initial pH was 8.3.

Table 1. Physico-chemical properties of the used dyes. Solubility data are from the references cited.

Dye	MW	Formula	Nature	Type	λmax	Solubility	Ref.
	(g mol^{-1})				(nm)	(g L^{-1})	
Methylene blue	319.85	$C_{16}H_{18}ClN_3S$	cationic	basic	664.5	43.6	[70]
Methyl orange	327.33	$C_{14}H_{14}N_3NaO_3S$	anionic	acid	464.0	5.0	[71]
Orange II	350.32	$C_{16}H_{11}N_2NaO_4S$	anionic	Acid	486.0	64.5	[72]
Reactive red 120	1338.1	$C_{44}H_{30}C_{l2}N_{14}O_{20}S_6$	anionic	acid	515.0	70.0	[73]

2.1.2. Solid Materials

Metallic Iron (Fe^0)

A total of 4 commercially available Fe^0 materials were selected and used in this study. The selection was based on their differential reactivity as determined in previous work [34]. The Fe^0 materials used were of different geometric shapes and sizes. These Fe^0 materials are referred to as: (i) ZVI1 is a material from iPutec GmbH Rheinfelden, Rheinfelden, Germany: (ii) ZVI2 is a directly reduced sponge iron material (DRI) from ISPAT GmbH, Hamburg, Germany; (iii) ZVI3 is scrap iron from the metal recycling company Metallaufbereitung Zwickau, Zwickau, Germany; and (iv) ZVI4 is a spherical iron sample from the Tongda Alloy Material Factory, Jinan, China. Table 2 summarizes the main characteristics of the 4 Fe^0 materials together with their iron content, as specified by the supplier. ZVI1 has been typically used by our research group since 2005 and represents the most widely used Fe^0 material for field applications in Europe [74]. Therefore, ZVI1 is used here as an operational reference.

Table 2. Code and main characteristics of the tested Fe^0 materials according to the supplier. n.s. = not specified; granular = mechanically broken pieces; sponge = particles with pitted surfaces; scrap = waste generated in any forms: spherical = standard sphere with a smooth surface. k_{AA} is the initial dissolution kinetics of each Fe^0 in a 2 mM ascorbic acid solution [34].

Code	Shape	Size	Color	k_{AA}	Fe	Supplier
		(mm)		(μg h^{-1})	(%)	
ZVI1	granular	0.05–5.00	black	13.2 ± 0.5	n.s.	iPutec GmbH
ZVI2	sponge	1.00–2.00	black	11.5 ± 1.3	90.0	ISPAT GmbH
ZVI3	scrap	0.05–2.00	black	12.3 ± 0.7	n.s.	Metallaufbereitung Zwickau
ZVI4	spherical	2.00	grey	2.8 ± 0.1	99.99	Tongda Alloy Material Factory

Sand

The sand used in this work was a commercial material for aviculture (parrot sand) ("Papageien sand" from RUT—Lehrte, Germany). "Papageien sand" was used as received without any further pre-treatment or characterization. The particle size varied between 0.5 and 2.0 mm. Sand was considered in this study because of its worldwide availability and its use as an additive in Fe^0/H_2O systems [50,54]. The high adsorption capacity of sand for cationic MB was systematically documented as early as 1955 [55].

2.2. Experimental Procedure

Batch experiments were performed under static conditions (no agitation) in assay tubes for 2 to 46 days. The batches consisted of 0.0 to 0.5 g of sand, 0.0 to 0.5 g of Fe^0, and mixtures thereof in 22.0 mL of a 10.0 mg L^{-1} of dye (MB, MO, OII, and RR 120) solution. Three different systems were investigated in parallel experiments for dye discoloration: (i) Fe^0 alone, (ii) sand alone, and (iii) Fe^0 + sand. The NaCl concentrations tested ranged from 0.0 to 40 g L^{-1}, corresponding to 0 to 24.3 g L^{-1} Cl^- (0 to 685 mM NaCl), without taking into account the Cl^- content of tap water (0.011–0.015 g L^{-1}). An operational reference (blank

experiment) was included in each experiment. Mixtures with Fe^0 characterize the effect of sand on the availability of "free" iron corrosion products and hence their effect on dye discoloration [54]. "Free" iron corrosion products are iron oxidhydroxides precipitating from the bulk solution and capable of fixing (enmeshing) contaminants [50]. The influence of different types of Fe^0 (ZVI1—ZVI4) on MB discoloration was also investigated. An additional set of dye discoloration experiments with MB and MO was performed by varying the Fe^0 loading (0.23 to 45 g L^{-1}) for two months.

The efficiency of each system in discoloring dyes was characterized at laboratory temperature (approximatively 22 °C). The initial pH value of the tap water was ~8.3. After equilibration, up to 5.0 mL of the supernatant solution was carefully collected for spectrophotometric analysis. Each experiment was performed in triplicate. Results are presented as means with the standard deviations (error bars) as a measure of data dispersion.

2.3. Analytical Procedure

Aqueous dye concentrations were determined using a Cary 50 UV–Vis spectrophotometer (Cary instruments, LabMakelaar Benelux B.V., Zevenhuizen, The Netherlands). The working wavelengths for MB, MO, OII, and RR 120 were 664.5, 464.0, 486.0, and 515.0 nm, respectively (Table 1). Cuvettes with a 1.0 cm light path were used. The spectrophotometer was calibrated for dye concentrations $\leq$ 10.0 mg L^{-1}. The pH value was measured with a combined glass electrode (WTW Co., Weinheim, Germany).

2.4. Expression of Experimental Results

In order to characterize the degree of dye discoloration of the tested systems, the treatment efficiency (E) was calculated (Equation (3)). After the determination of the residual dye concentration (C), the corresponding percentage discoloration (E value) was calculated as follows:

$$E = [1 - (C/C_0)] \times 100\% \quad (3)$$

where C_0 is the initial aqueous contaminant concentration (10.0 mg L^{-1} for each dye) and C is the corresponding concentration at the end of the experiment.

3. Results

3.1. Dye Discoloration in Fe^0/H_2O Systems

Figure 1 compares the extent of dye discoloration after 46 days under the experimental conditions: Quiescent batch tests with 4.5 g L^{-1} Fe^0 and 20 g L^{-1} sand. It can be seen that MB had the least extent of discoloration (55%) while Orange II had the best performance with an E value of 70%. These results confirm previous reports and are justified by the cationic nature of MB compared to the three other dyes, which are anionic (Table 1) [75–77]. In fact, the surface of FeCPs is positively charged just like the MB molecule, whereas anionic dyes (MO, orange II, and RR 120) (Table 1) are negatively charged and are more attracted to FeCPs [78,79]. The different behavior of anionic dyes may be explained by steric effects [77,80], which are not considered here.

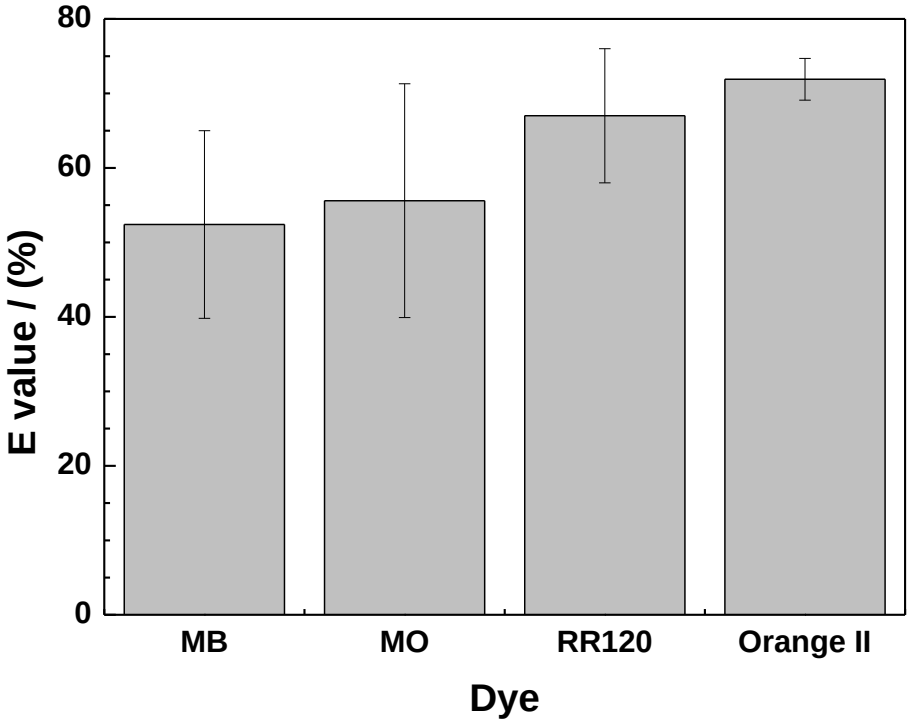


Figure 1. Degree of dye discoloration after 46 days in a Fe^0/H_2O system using ZVI1. Experimental conditions: m_{iron} = 0.1 g; m_{sand} = 0.5 g; $V_{solution}$ = 22 mL; [dye] = 10 mg L^{-1}; [NaCl] = 0.0 g L^{-1}.

When discussing the results in Figure 1, it should be kept in mind that the contact time (duration 46 days) was chosen so that the MB adsorption on sand would have already reached a pseudo-equilibrium [54]. In other words, changes in dye concentrations reflect the availability of free iron corrosion products for (i) the adsorption and co-precipitation of anionic dyes and (ii) the co-precipitation of all dyes (MB in particular). Clearly, the results in Figure 1 are the starting point for investigating the effects of NaCl addition on the performance of the given Fe^0/H_2O systems for dye discoloration (Section 3.3).

3.2. Influence of Salt Concentration on MB Discoloration in Fe^0/H_2O Systems

Figure 2 compares the time-dependent extent of MB discoloration under the experimental conditions for three different NaCl concentrations: 0.0, 8.0, and 40.0 g L^{-1}. It can be seen that for each contact time (i) MB discoloration is maximal in the NaCl free system (confirming the working hypothesis) and (ii) MB discoloration increases with increasing contact time. A closer look at the NaCl-containing systems shows that for t < 30 days, the 8 g L^{-1} NaCl system performed better than the 40 g L^{-1} system. Between 30 and 40 days, both systems performed similarly, and at t > 40 days, the 40 g L^{-1} NaCl system performed better than the 8 g L^{-1} system. However, both systems still performed lower than the NaCl-free system.

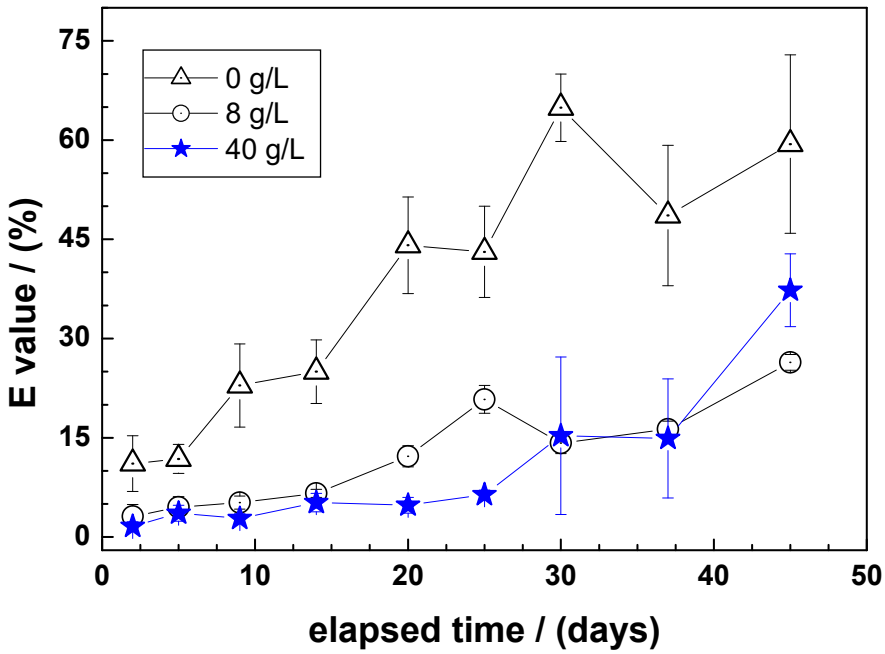


Figure 2. Time-dependent extent of methylene blue discoloration in Fe^0/sand systems as a function of the NaCl concentration using ZVI1. Experimental conditions: m_{iron} = 0.1 g; m_{sand} = 0.5 g; $V_{solution}$ = 22 mL; [MB] = 10 mg L^{-1}. The lines shown are not fitting functions, they simply connect the points for ease of visualization.

Figure 2 suggests that there is some ambivalence in the effects of Cl^- on the performance of Fe^0/H_2O systems for water treatment. The first reason may be an overall decrease in performance due to the absence or a reduced availability of FeCPs for contaminant adsorption and co-precipitation. This is evident when comparing NaCl free and NaCl-containing systems. Second, for the two NaCl-containing systems, there is first a decrease correlated with the amount of NaCl, then a phase in which both systems show the same performance. As the duration of the experiment increases, a stage is reached where the system with the higher NaCl level performs better than the others. Although this improved performance is still lower than that of the NaCl-free system, these results suggest that the improved MB discoloration performance for the 40 g L^{-1} NaCl system corresponds to the often reported improved performance of Fe^0/H_2O systems in the presence of Cl^- [59,60,64].

In this study, quiescent batch experiments in which diffusion transport is the dominant transport mechanism for dissolved species from the bulk solution to the vicinity of the Fe^0 surface have revealed the fundamental effects of the presence of Cl^- on the efficiency of Fe^0/H_2O systems for water treatment. Consistent with the chemistry of the system, Cl^- ions form stable dissolved complexes with Fe^{2+} and Fe^{3+}, delaying the formation of FeCPs for contaminant adsorption and/or co-precipitation. This observation clearly validates the working hypothesis: The presence of Cl^- delays the removal of contaminants in Fe^0/H_2O systems.

3.3. Influence of Salt Concentration on Dye Discoloration in Fe^0/H_2O Systems

Figure 3 summarizes the extent of dye discoloration after 46 days as the NaCl concentration varied from 0 to 40 g L^{-1}. It can be seen that the presence of Cl^- ions inhibits the discoloration of all dyes. The first experimental point at 0 g L^{-1} NaCl corresponds to the discussion in Section 3.1 (Figure 1), where the dye discoloration decreased in the order: OII > MO > RR120 > MB. A monotonic decrease in E values with increasing NaCl concentration is then observed for [NaCl] < 30 g L^{-1}, alongside a slight increase for [NaCl] = 40 g L^{-1}. This ambivalent situation is similar to that observed in the time-dependent study with

MB (Section 3.2) and is related to the relative amounts of Fe(II) and Fe(III) chlorocomplexes and the availability of FeCPs (Equation (2)). Taken together, the results presented in Figure 1 through 3 suggest that it is possible to properly design a Fe^0-based remediation system that takes advantage of the enhanced iron corrosion in the presence of Cl^- ions. However, this does not mean that Cl^- ions generally increase the efficiency of Fe^0/H_2O systems. Similar results have been obtained with hybrid Fe^0/aggregate systems, including Fe^0/MnO_2 [43–45,77,81], Fe^0/pumice [18,82], and Fe^0/sand [30,52,79,83]. In other words, designing a sustainable Fe^0 remediation system in a saline environment requires a careful consideration of the balance between acceptable Cl^- concentration and contaminant removal efficiency for each Fe^0 material.

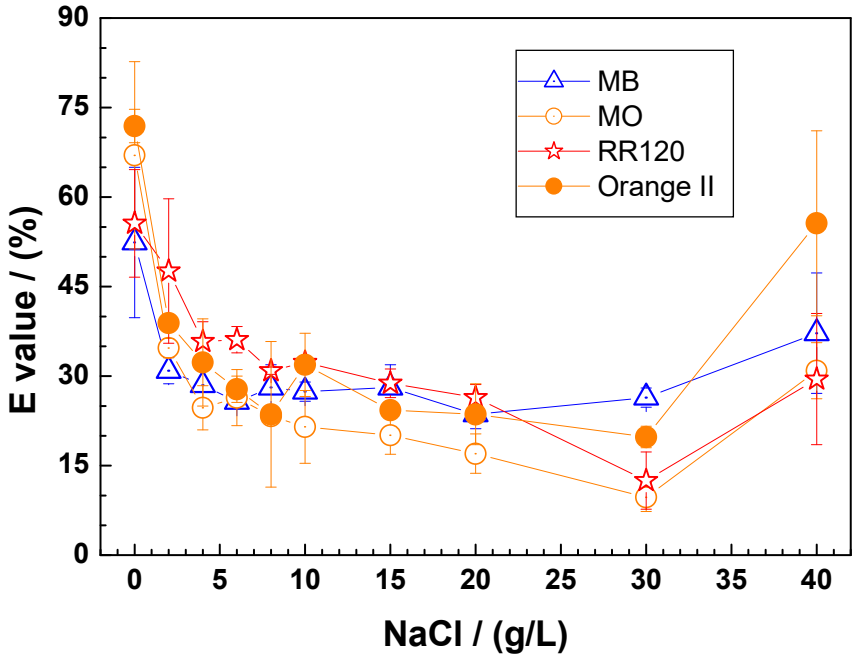


Figure 3. Extent of dye discoloration after 46 days as a function of the NaCl concentration using ZVI1. Experimental conditions: m_{iron} = 0.1 g; m_{sand} = 0.5 g; $V_{solution}$ = 22 mL; [dye] = 10 mg L^{-1}. The lines shown are not fitting functions, they simply connect the points for ease of visualization.

3.4. Influence of Fe^0 Dosage on Dye Discoloration in Fe^0/H_2O Systems

Figure 4 summarizes the effect of 0.0 to 45.0 g L^{-1} Fe^0 on the extent of MB and MO discoloration over 46 days. The percentage discoloration of both dyes increased with increasing Fe^0 dosage, while the presence of salt (NaCl) typically reduced the extent of dye discoloration. The point at 0.0 g L^{-1} Fe^0 (sand only) corresponds to the Fe^0 free system in which dye discoloration is mediated solely by electrostatic interactions at the negatively charged sand surface [50,55]. Figure 4a shows that more than 20% of MB is discolored in the pure sand system, while there was no MO discoloration (E = 0%—Figure 4b). Another feature of Figure 4a is that the presence of salt reduces the extent of MB discoloration by sand. In the presence of Fe^0, decrease MB discoloration is also due to the increased availability of Fe^{2+} and Fe^{3+} ions, which are concurrent with MB (also positively charged) for adsorption onto the sand surface [78].

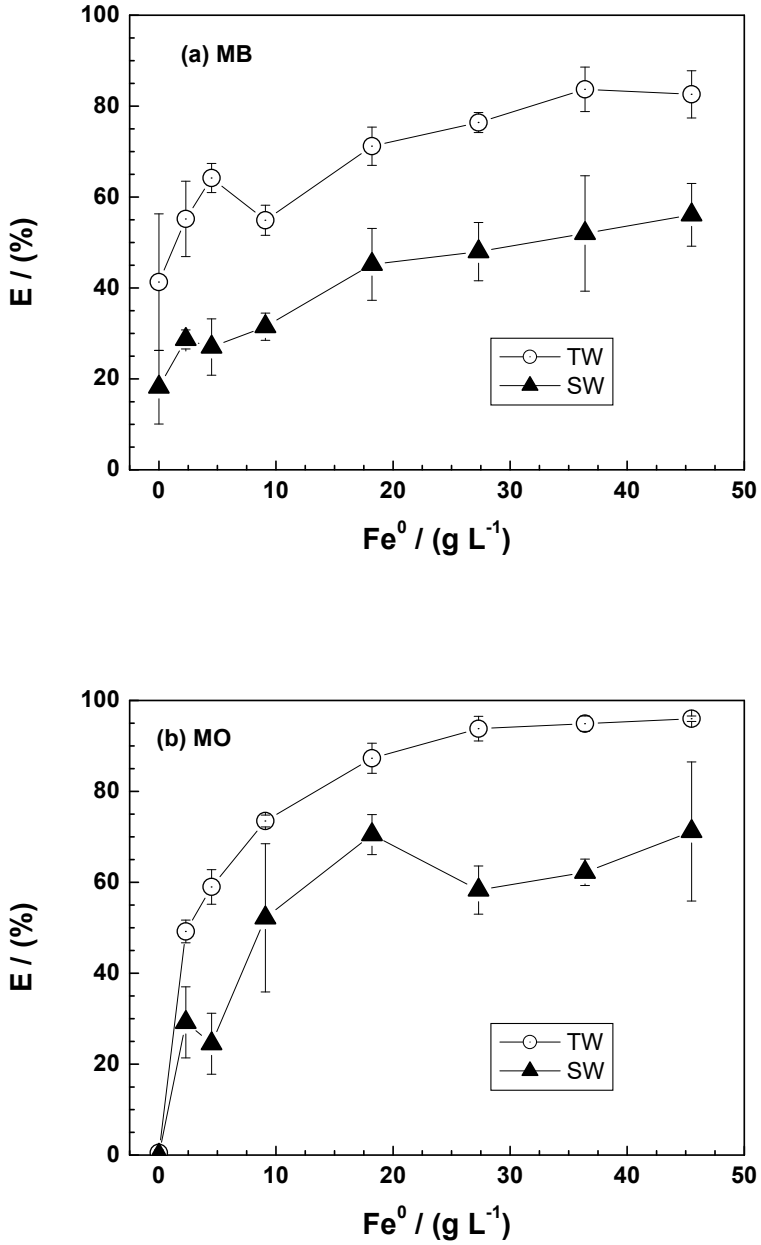


Figure 4. Extent of dye discoloration after 46 days as a function of the Fe^0 dosage for methylene blue (**a**) and methyl orange (**b**) using ZVI1. Experimental conditions: m_{iron} = 0.1 g; m_{sand} = 0.5 g; $V_{solution}$ = 22 mL; [dye] = 10 mg L^{-1}. The lines shown are not fitting functions, they simply connect the points for ease of visualization.

For Fe^0 dosages between 0 and 45 g L^{-1}, there is an increase in dye discoloration efficiency with increasing iron dosage (Figure 4a,b). This is primarily due to the availability of more active binding sites as a result of continuous iron corrosion, which produces solid iron corrosion products (FeCPs) for dye adsorption and co-precipitation. However, the discoloration percentage for both dyes becomes almost constant for [Fe^0] > 20.0 g L^{-1}. This behavior suggests a "splitting effect of the concentration gradient" between FeCPs and dye molecules [84]. The different discoloration efficiencies of MB and MO as a function of the amount of FeCPs available are essentially due to differences in chemical structure, molecular size, and FeCPs–dye interactions [50,55,84].

3.5. Influence of Fe^0 Type on Dye Discoloration in Fe^0/H_2O Systems

Figure 5 summarizes the extent of MB and discoloration after 46 days with four different Fe^0 materials in tap water ([NaCl] = 0 g L^{-1}) and in salt water ([NaCl] = 40 g L^{-1}). It can be seen that for all the 4 Fe^0 materials tested, the dye discoloration decreases in salt water compared to tap water, confirming the observations in Section 3.4 and further validating the working hypothesis.

For MB (Figure 5a), the most significant TW vs. SW variability between replicates was observed for ZVI1 (error bars), while the lowest was recorded for ZVI4. Considering the absolute values, the following increasing order of efficiency is observed: ZVI4 > ZVI3 > ZVI2 > ZVI1. This ranking confirms the information from the k_{AA} values (Table 2), showing that ZVI4 is significantly less reactive than the other three materials [9]. Another feature of Figure 5a is that ZVI4 performed only slightly better than sand alone in SW and TW. Based on the information in Figure 5a, ZVI1 can be recommended as the most reactive material, while ZVI2 and ZVI3 are very close in their efficiency for MB discoloration. The results of MO discoloration (Figure 5b) confirm the trend observed in Figure 5a, with the exception that ZVI1 has a significantly lower efficiency in both TW and SW. While this difference is difficult to justify, the overall results reaffirm the importance of characterizing the diversity among the Fe^0 materials of environmental interest [85,86].

Despite a growing interest in the applications of Fe^0 for environmental remediation [14,22,23] and safe drinking water supply [87–90], little progress has been made in characterizing the variability in reactivity among Fe^0 samples from different sources [19,34,86,91,92]. The most important lesson from Figure 5 is that the extent to which saltwater affects the performance of a Fe^0/H_2O system depends on the used Fe^0 source used (Fe^0 quality). In particular, one investigator using ZVI4 might conclude that Cl^- ions have no effect on Fe^0 efficiency, while a colleague working under similar conditions using ZVI1 or ZVI2 would come to a different conclusion. As discussed by several authors, the diversity of contaminants and Fe^0 materials, as well as the lack of unified or standardized experimental procedures are the three most important factors hindering the progress of knowledge in the design of sustainable Fe^0-based remediation systems [17,19,30,77,92].

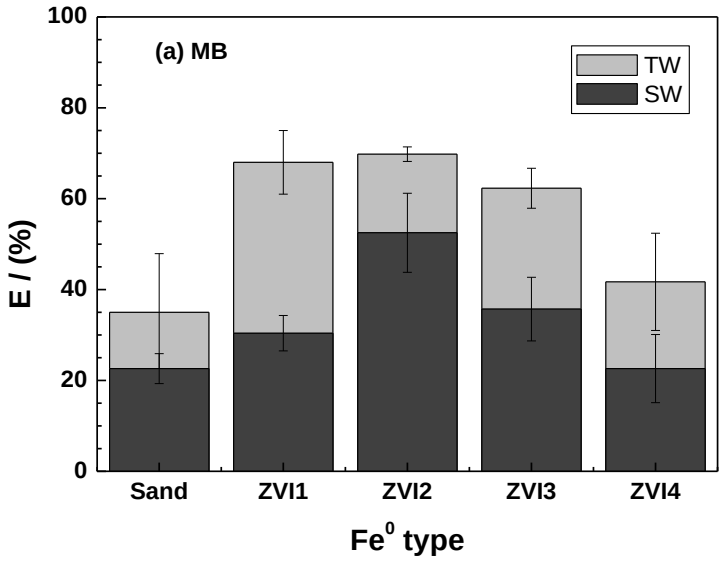


Figure 5. *Cont.*

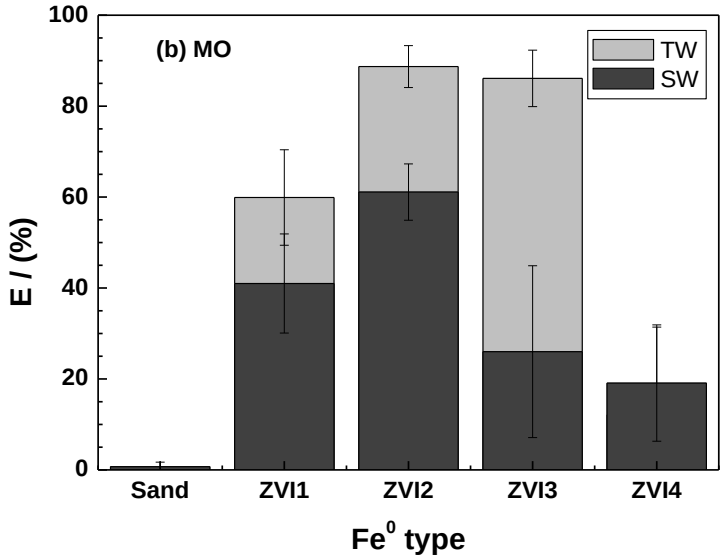


Figure 5. Extent of MB discoloration after 46 days as a function of the Fe^0 type for methylene blue (**a**) and methyl orange (**b**). Experimental conditions: m_{iron} = 0.1 g; m_{sand} = 0.5 g; $V_{solution}$ = 22 mL; [MB] = 10 mg L^{-1}.

4. Discussion

The results presented here clearly demonstrate that any Cl^- addition hinders the process of contaminant removal in Fe^0/H_2O systems. The results clearly contradict published findings over the past 20 years which claim that Cl^- addition typically enhances water treatment with granular Fe^0 [59,64,86,93]. For example, Kim et al. [59] tested halide salts to sustain the Fe^0 efficiency for explosive "degradation" and concluded that Fe^0 PRBs "installed in aquifers with chloride-rich groundwater are likely to perform and maintain reactivity better than those installed in aquifers with low chloride concentrations". Many other researchers have reached similar conclusions for chloride-rich wastewater [63,93–95]. The question is—how can both views be reconciled?

Since the first peer-reviewed publications on Fe^0 for groundwater remediation in 1994 [35,96–98], researchers have been trying to solve the problem of avoiding or delaying Fe^0 passivation, commonly referred to as "reactivity loss" [11,99,100]. An applicable solution has been the use of chlorides (e.g., NaCl, KCl) as pitting corrosion promoters to avoid or destroy the oxide layer formed on the Fe^0 surface [64]. Avoiding, breaking, or eliminating these oxide scales allows for the full utilization of the reductive capacity of the Fe^0 materials used, as predicted by the thermodynamics of the Fe^{II}/Fe^0 redox couple (E^0 = −0.44 V). Indeed, despite NaCl concentrations as high as 40 g L^{-1} (685 mM Cl^-), no improvement in dye discoloration was observed here, even for MO and orange II, which are potentially reduced by Fe^0 [76,80].

The addition of chloride (e.g., KCl, NaCl) to Fe^0/H_2O systems is generally regarded as the addition of a "corrosion promoter" to accelerate the degradation of contaminants during water treatment [59,93,101,102]. Hernandez et al. [93] theorized that corrosion promoters improve the performance of Fe^0/H_2O systems by (i) accelerating "electron generation" from Fe^0, (ii) creating new reactive sites on the Fe^0 surface during water treatment, and (iii) minimizing surface passivation. The results of their experiments with 0.3 mM and 3 mM Cl^- for "TNT degradation" were considered a validation of their concept. Subsequent investigators have reached similar conclusions [59,102], so that it appears to be established that the well-documented corrosion-promoting effects of Cl^- can be randomly exchanged for accelerated contaminant degradation in $Fe^0/Cl^-/H_2O$ systems. However, using nanoscale Fe^0, Hwang et al. [54] clearly observed an inhibition of nitrate reduction in Fe^0/H_2O systems after the addition of NaCl. These authors explained their observations by chloride adsorption on the Fe^0 surface, using NaCl concentrations of up to 12 g L^{-1}

(205 mM Cl^-). The present work used higher and lower NaCl concentrations (Table 3) but gave different reasons for the inhibition of the four probe substances.

Table 3. Selected experimental conditions from published papers on the effect of chloride ions on the efficiency of water remediation using Fe^0 materials; mFe^0 = macroscale ZVI, nFe^0 = nanoscale ZVI, sFe^0 = sulfidated ZVI.

Fe^0 Material					Mixing		
Nature	**Dose**	**V**	**Contaminant**	**(Chloride)**	**Nature**	**Speed**	**Reference**
	($g\ L^{-1}$)	(mL)		(mM)		(rpm)	
mFe^0	1–2.5	5	Selenate	n.s.	n.s.	100	[103]
mFe^0	1	5	RDX	n.s.	shaking	100	[104]
mFe^0	1.25	25	selenate	10	shaking	180	[94]
mFe^0	10	25	RX	0.5, 5.0, 50	shaking	n.s.	[59]
nFe^0	1.25	800	Nitrate	0 to 342	stirring	200	[64]
mFe^0	2	100	Cr(VI)	10	n.s	n.s	[95]
mFe^0	2.5	100	Phosphate	10	n.s.	165	[105]
sFe^0	0.5	500	Selenate	10	stirring	400	[61]
mFe^0	2	200	Silicate	n.s.	stirring	200	[106]
nFe^0/Fe_3O_4	0.25	1000	Arsenate	2.8	stirring	1000	[107]
mFe^0	0–45	22	Dyes	0 to 685	none	0	This study

Table 3 summarizes the experimental conditions of selected publications on the effects of NaCl on the performance of Fe^0/H_2O batch systems. It can be clearly seen that there is a large variability in the experimental parameters used. This includes: (i) the type of the Fe^0 materials (mFe^0, nFe^0, composites), (ii) the Fe^0 dosage (0 to 45 $g\ L^{-1}$), (iii) the volume of the solution (5 to 1000 mL), (iv) the type of the contaminant and even its concentration (not shown), (v) the Cl^- concentrations (0 to 685 mM), and (vi) the type and intensity of mixing. All of these parameters have been shown to individually significantly affect the remediation efficiency of Fe^0/H_2O systems [13,20,30,33,108,109]. However, their effects are interdependent, and it is almost impossible to assess the contribution of each parameter as a stand-alone variable. Table 3 shows that this study differs from others in two ways: (i) quiescent batch experiments were performed and (ii) the widest window of Cl^- concentrations to date was tested. The latter aspect is very important, as Hwang et al. [64] rationalized the decrease in aqueous nitrate removal by nano-Fe^0 by the higher Cl^- content.

This study has not confirmed the different effects of Cl^- depending on its concentration. Hwang et al. [64] reported that at low concentrations (0–3 $g\ L^{-1}$ NaCl), the efficiency of the system decreased only during the initial reaction period and then "increased after a certain time". The efficiency at high Cl^- concentrations (3–20 $g\ L^{-1}$) decreased significantly "due to the inhibition effect of the electrolyte". This statement contradicts the electrochemistry of the system. In fact, in an electrochemical reaction, the contribution of the electrolyte is to modify the ionic transport of anodic species (here Fe^{2+}) not to influence a cathodic reaction (electron transfer to NO_3^-). Accordingly, the results of Hwang et al. [64] explicitly refute the notion that nitrate reduction is mediated by any electrons of Fe^0. In other words, the results presented here elegantly confirm that Fe^0 is a generator of contaminant scavengers [33,53,54]. The presence of NaCl delays the precipitation of iron oxides and hydroxides, thus delaying the decontamination process. This was observed for all four dyes and at all NaCl concentrations. It is recalled that the dyes used have different redox affinities to Fe^0 ($E^0 = -0.44$ V) and different adsorptive affinities to positively charged iron corrosion products [110–112]. The discoloration results reflect only the difference in adsorptive adsorption affinity, confirming reports that Fe^0/H_2O systems are ion-selective [75,76,113].

The final important point is to explain why improved decontamination efficiency has been documented for some Fe^0/H_2O systems [64,114]. Fe^0 would "passivate" earlier without Cl^- addition. Due to the high solubility of Fe(II) and Fe(III) chlorides relative to iron hydroxides, Cl^- addition sustains Fe^0 corrosion and produces more contaminant scavengers because Fe^0 is in large stoichiometric excess. All of these reactions are enhanced by mixing operations, such as shaking and stirring (Table 3). A similar situation has been reported for the addition of MnO_2 to Fe^0 and Fe^0 amendment with sand [43–45,81]. Here, MnO_2 promotes the Fe^{2+} oxidation and increases the formation of contaminant scavengers (FeCPs) compared to the pure Fe^0 system [77,110]. Obviously, there is no contradiction between the retardation of contaminant removal in the presence of chloride ions and the improved efficiency of the same systems compared to the operational reference (Cl^- free Fe^0/H_2O).

5. Conclusions

The view that NaCl addition initially prevents contaminant removal in Fe^0/H_2O systems is consistent with (i) the science of iron corrosion (e.g., solubility of Fe ions) and (ii) many experimental observations related to dye discoloration. However, this does not contradict the well-documented fact that some Fe^0-based filters fed with chloride-rich waters perform better than those fed with fresh water. In addition, the results presented here confirm the key role of iron corrosion products (e.g., hydroxides and oxides) in the decontamination process of Fe^0-based systems, including decentralized filters, such as household Kanchan filters in Southeast Asia. This observation suggests that the periodic flushing of Kanchan filters with NaCl solutions (e.g., table salt) is another potentially powerful tool for maintaining their efficiency. Thus, the results presented here can help developing countries in their efforts to meet the Sustainable Development Goal (SDG) Target 6.1, which aims to achieve universal and equitable access to safe and affordable drinking water for all by 2030.

Author Contributions: Conceptualization: R.T., X.C., M.X. and C.N.; methodology, R.T., X.C., M.X. and C.N.; writing—original draft preparation, R.T., X.C., M.X., W.G. and C.N.; writing—review and editing, C.N., R.H., W.G. and H.R. All authors have read and agreed to the published version of the manuscript.

Funding: This research received no external funding.

Data Availability Statement: Data are available on request.

Acknowledgments: The manuscript was improved thanks to the insightful comments of anonymous reviewers for *Water*. We acknowledge support by the German Research Foundation and the Open Access Publication Funds of the Göttingen University.

Conflicts of Interest: The authors declare no conflict of interest.

References

1. Ranjan, S.P.; Kazama, S.; Sawamoto, M. Effects of climate and land use changes on groundwater resources in coastal aquifers. *J. Environ. Manag.* **2006**, *80*, 25–35. [CrossRef] [PubMed]
2. Gain, A.K.; Wada, Y. Assessment of future water scarcity at different spatial and temporal scales of the Brahmaputra River Basin. *Water Resour. Manag.* **2014**, *28*, 999–1012. [CrossRef]
3. Abd-Elaty, I.; Straface, S.; Kuriqi, A. Sustainable saltwater intrusion management in coastal aquifers under climatic changes for humid and hyper-arid regions. *Ecol. Eng.* **2021**, *171*, 106382. [CrossRef]
4. Agoubi, B. A review: Saltwater intrusion in North Africa's coastal areas—Current state and future challenges. *Environ. Sci. Pollut. Res.* **2021**, *28*, 17029–17043. [CrossRef] [PubMed]
5. Passerat, J.; Ouattara, N.K.; Mouchel, J.-M.; Rocher, V.; Servais, P. Impact of an intense combined sewer overflow event on the microbiological water quality of the Seine River. *Water Res.* **2011**, *45*, 893–903. [CrossRef] [PubMed]
6. Sambito, M.; Freni, G. Strategies for improving optimal positioning of quality sensors in urban drainage systems for non-conservative contaminants. *Water* **2021**, *13*, 934. [CrossRef]
7. Banerji, T.; Chaudhari, S. A cost-effective technology for arsenic removal: Case study of zerovalent iron-based IIT Bombay arsenic filter in West Bengal. In *Water and Sanitation in the New Millennium*; Nath, K., Sharma, V., Eds.; Springer: New Delhi, India, 2017.

8. Antia, D.D.J. Hydrodynamic decontamination of groundwater and soils using ZVI. *Water* **2023**, *15*, 540. [CrossRef]
9. Xin, J.; Tang, F.; Yan, J.; La, C.; Zheng, X.; Liu, W. Investigating the efficiency of microscale zero valent iron-based in situ reactive zone (mZVI-IRZ) for TCE removal in fresh and saline groundwater. *Sci. Total Environ.* **2018**, *626*, 638–649. [CrossRef]
10. Gao, C.; Wang, B.; Xingchun Li, X.; Zhang, Y.; Qu, T.; Du, X.; Zheng, J.; Feng, J. Removal of Cr(VI) by hollow micron zero-valent iron in groundwater containing different ions: Mechanisms and mineralized products. *Proc. Saf. Environ. Protect.* **2023**, *173*, 614–626. [CrossRef]
11. Henderson, A.D.; Demond, A.H. Long-term performance of zero-valent iron permeable reactive barriers: A critical review. *Environ. Eng. Sci.* **2007**, *24*, 401–423. [CrossRef]
12. Gheju, M. Hexavalent chromium reduction with zero-valent iron (ZVI) in aquatic systems. *Water Air Soil Pollut.* **2011**, *222*, 103–148. [CrossRef]
13. Ghauch, A. Iron-based metallic systems: An excellent choice for sustainable water treatment. *Freib. Online Geosci.* **2015**, *32*, 1–80.
14. Guan, X.; Sun, Y.; Qin, H.; Li, J.; Lo, I.M.C.; He, D.; Dong, H. The limitations of applying zero-valent iron technology in contaminants sequestration and the corresponding countermeasures: The development in zero-valent iron technology in the last two decades (1994–2014). *Water Res.* **2015**, *75*, 224–248. [CrossRef] [PubMed]
15. Gheju, M. Progress in understanding the mechanism of Cr^{VI} Removal in Fe^0-based filtration systems. *Water* **2018**, *10*, 651. [CrossRef]
16. Antia, D.D.J. Water treatment and desalination using the eco-materials n-Fe^0 (ZVI), n-Fe_3O_4, n-$Fe_xO_yH_z[mH_2O]$, and n-$Fe_x[Cation]_nO_yH_z[Anion]_m$ [rH_2O]. In *Handbook of Nanomaterials and Nanocomposites for Energy and Environmental Applications*; Kharissova, O.V., Martínez, L., Kharisov, B., Eds.; Springer Nature: Cham, Switzerland, 2020. [CrossRef]
17. Cao, V.; Bakari, O.; Kenmogne-Tchidjo, J.F.; Gatcha-Bandjun, N.; Ndé-Tchoupé, A.I.; Gwenzi, W.; Njau, K.N.; Noubactep, C. Conceptualizing the Fe^0/H_2O system: A call for collaboration to mark the 30th anniversary of the Fe^0-based permeable reactive barrier technology. *Water* **2022**, *14*, 3120. [CrossRef]
18. Bilardi, S.; Calabrò, P.S.; Moraci, N. A review of the hydraulic performance of permeable reactive barriers based on granular zero valent iron. *Water* **2023**, *15*, 200. [CrossRef]
19. Cui, X.; Xiao, M.; Tao, R.; Hu, R.; Ruppert, H.; Gwenzi, W.; Noubactep, C. Developing the ascorbic acid test: A candidate standard tool for characterizing the intrinsic reactivity of metallic iron for water remediation. *Water* **2023**, *15*, 1930. [CrossRef]
20. Lan, L.E.; Reina, F.D.; De Seta, G.E.; Meichtry, J.M.; Litter, M.I. Comparison between different technologies (zerovalent iron, coagulation-flocculation, adsorption) for arsenic treatment at high concentrations. *Water* **2023**, *15*, 1481. [CrossRef]
21. Lawrinenko, M.; Kurwadkar, S.; Wilkin, R.T. Long–term performance evaluation of zero-valent iron amended permeable reactive barriers for groundwater remediation—A mechanistic approach. *Geosci. Front.* **2023**, *14*, 101494. [CrossRef]
22. Plessl, K.; Russ, A.; Vollprecht, D. Application and development of zero-valent iron (ZVI) for groundwater and wastewater treatment. *Int. J. Environ. Sci. Technol.* **2022**, *20*, 6913–6928. [CrossRef]
23. Singh, R.; Chakma, S.; Birke, V. Performance of field-scale permeable reactive barriers: An overview on potentials and possible implications for in-situ groundwater remediation applications. *Sci. Total Environ.* **2023**, *858*, 158838. [CrossRef] [PubMed]
24. Cundy, A.B.; Hopkinson, L.; Whitby, R.L.D. Use of iron-based technologies in contaminated land and groundwater remediation: A review. *Sci. Total Environ.* **2008**, *400*, 42–51. [CrossRef] [PubMed]
25. Thiruvenkatachari, R.; Vigneswaran, S.; Naidu, R. Permeable reactive barrier for groundwater remediation. *J. Ind. Eng. Chem.* **2008**, *14*, 145–156. [CrossRef]
26. Chen, Q.; Fan, G.; Na, W.; Liu, J.; Cui, J.; Li, H. Past, present, and future of groundwater remediation research: A scientometric analysis. *Int. J. Environ. Res. Public Health* **2019**, *16*, 3975. [CrossRef]
27. Li, X.; Li, Z.; Du, C.; Tian, Z.; Zhu, Q.; Li, G.; Shen, Q.; Li, C.; Li, J.; Li, W.; et al. Bibliometric analysis of zerovalent iron particles research for environmental remediation from 2000 to 2019. *Environ. Sci. Pollut. Res.* **2021**, *28*, 4200–34210. [CrossRef]
28. Noubactep, C. Metallic iron for environmental remediation: A review of reviews. *Water Res.* **2015**, *85*, 114–123. [CrossRef]
29. Antia, D.D.J. Remediation of saline wastewater producing a fuel gas containing alkanes and hydrogen using zero valent iron (Fe^0). *Water* **2022**, *14*, 1926. [CrossRef]
30. Gheju, M.; Balcu, I. Effect of sand co-presence on Cr^{VI} removal in Fe^0-H_2O system. *Water* **2023**, *15*, 777. [CrossRef]
31. Lawrinenko, M.; Kurwadkar, S.; Wilkin, R.T. Responses to comments by Dr. Noubactep. *Geosci. Front.* **2023**, *15*, 101494. [CrossRef]
32. Noubactep, C. Comments on "Long-term performance evaluation of zero-valent iron amended permeable reactive barriers for groundwater remediation—A mechanistic approach" by Lawrinenko et al., Geoscience Frontiers 14 (2023) 101494. *Geosci. Front.* **2023**, *15*, 101582. [CrossRef]
33. Hu, R.; Gwenzi, W.; Sipowo, T.R.; Ndé-Tchoupé, A.I.; Cao, V.; Gwenzi, W.; Noubactep, C. Metallic iron for environmental remediation: The fallacy of the electron efficiency concept. *Front. Environ. Chem.* **2021**, *2*, 677813. [CrossRef]
34. Ndé-Tchoupé, A.I.; Hu, R.; Gwenzi, W.; Nassi, A.; Noubactep, C. Characterizing the reactivity of metallic iron for water treatment: H_2 evolution in H_2SO_4 and uranium removal efficiency. *Water* **2020**, *12*, 1523. [CrossRef]
35. Matheson, L.J.; Tratnyek, P.G. Reductive dehalogenation of chlorinated methanes by iron metal. *Environ. Sci. Technol.* **1994**, *28*, 2045–2053. [CrossRef] [PubMed]
36. Warren, K.D.; Arnold, R.G.; Bishop, T.L.; Lindholm, L.C.; Betterton, E.A. Kinetics and mechanism of reductive dehalogenation of carbon tetrachloride using zero-valence metals. *J. Hazard. Mater.* **1995**, *41*, 217–227. [CrossRef]

37. Fiedor, J.N.; Bostick, W.D.; Jarabek, R.J.; Farrel, J. Understanding the mechanism, of uranium removal from groundwater by zero-valent iron using X-ray photoelectron spectroscopy. *Environ. Sci. Technol.* **1998**, *32*, 1466–1473. [CrossRef]
38. Farrell, J.; Bostick, W.D.; Jarabeck, R.J.; Fiedor, J.N. Uranium removal from ground water using zero valent iron media. *Ground Water* **1999**, *34*, 618–624. [CrossRef]
39. Qiu, S.R.; Lai, H.-F.; Roberson, M.J.; Hunt, M.L.; Amrhein, C.; Giancarlo, L.C.; Flynn, G.W.; Yarmoff, J.A. Removal of contaminants from aqueous solution by reaction with iron surfaces. *Langmuir* **2000**, *16*, 2230–2236. [CrossRef]
40. Lavine, B.K.; Auslander, G.; Ritter, J. Polarographic studies of zero valent iron as a reductant for remediation of nitroaromatics in the environment. *Microchem. J.* **2001**, *70*, 69–83. [CrossRef]
41. Jiao, Y.; Qiu, C.; Huang, L.; Wu, K.; Ma, H.; Chen, S.; Ma, L.; Wu, L. Reductive dechlorination of carbon tetrachloride by zero-valent iron and related iron corrosion. *Appl. Catal. B Environ.* **2009**, *91*, 434–440. [CrossRef]
42. Ebelle, T.C.; Makota, S.; Tepong-Tsindé, R.; Nassi, A.; Noubactep, C. Metallic iron and the dialogue of the deaf. *Fresenius Environ. Bull.* **2019**, *28*, 8331–8340.
43. Ghauch, A.; Abou Assi, H.; Bdeir, S. Aqueous removal of diclofenac by plated elemental iron: Bimetallic systems. *J. Hazard. Mater.* **2010**, *182*, 64–74. [CrossRef] [PubMed]
44. Ghauch, A.; Abou Assi, H.; Baydoun, H.; Tuqan, A.M.; Bejjani, A. Fe^0-based trimetallic systems for the removal of aqueous diclofenac: Mechanism and kinetics. *Chem. Eng. J.* **2011**, *172*, 1033–1044. [CrossRef]
45. Gheju, M.; Balcu, I. Sustaining the efficiency of the Fe(0)/H_2O system for Cr(VI) removal by MnO_2 amendment. *Chemosphere* **2019**, *214*, 389–398. [CrossRef] [PubMed]
46. Devlin, J.F.; Klausen, J.; Schwarzenbach, R.P. Kinetics of nitroaromatic reduction on granular iron in recirculating batch experiments. *Environ. Sci. Technol.* **1998**, *32*, 1941–1947. [CrossRef]
47. Devlin, J.F.; Allin, K.O. Major anion effects on the kinetics and reactivity of granular iron in glass-encased magnet batch reactor experiments. *Environ. Sci. Technol.* **2005**, *39*, 1868–1874. [CrossRef]
48. Noubactep, C. Processes of contaminant removal in "Fe^0–H_2O" systems revisited. The importance of co-precipitation. *Open Environ. Sci.* **2007**, *1*, 9–13. [CrossRef]
49. Noubactep, C. A critical review on the mechanism of contaminant removal in Fe^0–H_2O systems. *Environ. Technol.* **2008**, *29*, 909–920. [CrossRef]
50. Miyajima, K. Optimizing the design of metallic iron filters for water treatment. *Freib. Online Geosci.* **2012**, *32*, 1–60.
51. Miyajima, K.; Noubactep, C. Effects of mixing granular iron with sand on the efficiency of methylene blue discoloration. *Chem. Eng. J.* **2012**, *200–202*, 433–438. [CrossRef]
52. Btatkeu-K, B.D.; Tchatchueng, J.B.; Noubactep, C.; Caré, S. Designing metallic iron based water filters: Light from methylene blue discoloration. *J. Environ. Manag.* **2016**, *166*, 567–573. [CrossRef]
53. Konadu-Amoah, B.; Ndé-Tchoupé, A.I.; Hu, R.; Gwenzi, W.; Noubactep, C. Investigating the Fe^0/H_2O systems using the methylene blue method: Validity, applications and future directions. *Chemosphere* **2021**, *291*, 132913. [CrossRef] [PubMed]
54. Konadu-Amoah, B.; Hu, R.; Cui, X.; Tao, R.; Ndé-Tchoupé, A.I.; Gwenzi, W.; Noubactep, C. Characterizing the process of phosphate removal in Fe^0/H_2O systems. *Chem. Eng. J.* **2023**, *465*, 143042. [CrossRef]
55. Mitchell, G.; Poole, P.; Segrove, H.D. Adsorption of methylene blue by high-silica sands. *Nature* **1955**, *176*, 1025–1026. [CrossRef]
56. Tepong-Tsindé, R.; Phukan, M.; Nassi, A.; Noubactep, C.; Ruppert, H. Validating the efficiency of the MB discoloration method for the characterization of Fe^0/H_2O systems using accelerated corrosion by chloride ions. *Chem. Eng. J.* **2015**, *279*, 353–362. [CrossRef]
57. Klausen, J.; Ranke, J.; Schwarzenbach, R. Influence of solution composition and column aging on the reduction of nitroaromatic compounds by zero-valent iron. *Chemosphere* **2001**, *44*, 511–517. [CrossRef]
58. Su, C.; Puls, R.W. Arsenate and arsenite removal by zerovalent iron: Effects of phosphate, silicate, carbonate, borate, sulfate, chromate, molybdate, and nitrate, relative to chloride. *Environ. Sci. Technol.* **2001**, *35*, 4562–4568. [CrossRef]
59. Kim, J.S.; Shea, P.J.; Yang, J.E.; Kim, J.E. Halide salts accelerate degradation of high explosives by zerovalent iron. *Environ. Pollut.* **2007**, *147*, 634–641. [CrossRef] [PubMed]
60. Pullin, H.; Crane, R.A.; Morgan, D.J.; Scott, T.B. The effect of common groundwater anions on the aqueous corrosion of zero-valent iron nanoparticles and associated removal of aqueous copper and zinc. *J. Environ. Chem. Eng.* **2017**, *5*, 1166–1173. [CrossRef]
61. Ling, J.; Qiao, J.; Song, Y.; Sun, Y. Influence of coexisting ions on the electron efficiency of sulfidated zerovalent iron toward Se(VI) removal. *Chem. Eng. J.* **2019**, *378*, 122124. [CrossRef]
62. Li, R.; Li, Q.; Zhang, W.; Sun, X.; Li, J.; Shen, J.; Han, W. Low dose of sulfur-modified zero-valent iron for decontamination of trace Cd (II)-complexes in high-salinity wastewater. *Sci. Total Environ.* **2021**, *793*, 148579. [CrossRef]
63. Sun, Y.; Li, J.; Huang, T.; Guan, X. The influences of iron characteristics, operating conditions and solution chemistry on contaminants removal by zero-valent iron: A review. *Water Res.* **2016**, *100*, 277–295. [CrossRef] [PubMed]
64. Hwang, Y.; Kim, D.; Shin, H.-S. Inhibition of nitrate reduction by NaCl adsorption on a nano-zero-valent iron surface during a concentrate treatment for water reuse. *Environ. Technol.* **2015**, *36*, 1178–1187. [CrossRef] [PubMed]
65. Sun, Y.; Lei, C.; Khan, E.; Chen, S.S.; Tsang, D.C.W.; Ok, Y.S.; Lin, D.; Feng, Y.; Li, X.D. Nanoscale zero-valent iron for metal/metalloid removal from model hydraulic fracturing wastewater. *Chemosphere* **2017**, *176*, 315–323. [CrossRef] [PubMed]
66. Antia, D.D.J. ZVI (Fe^0) desalination: Catalytic partial desalination of saline aquifers. *Appl. Water Sci.* **2018**, *8*, 71. [CrossRef]

67. Ahmed, N.; Vione, D.; Rivoira, L.; Carena, L.; Castiglioni, M.; Bruzzoniti, M.C. A review on the degradation of pollutants by fenton-like systems based on zero-valent iron and persulfate: Effects of reduction potentials, pH, and anions occurring in waste waters. *Molecules* **2021**, *26*, 4584. [CrossRef]
68. Whitney, W.R. The corrosion of iron. *J. Am. Chem. Soc.* **1903**, *25*, 394–406. [CrossRef]
69. Wang, D.; Gilliland, S.E., III; Yi, X.; Logan, K.; Heitger, D.R.; Lucas, H.R.; Wang, W.N. Iron mesh-based metal organic framework filter for efficient arsenic removal. *Environ. Sci. Technol.* **2018**, *52*, 4275–4284. [CrossRef]
70. Khan, I.; Saeed, K.; Zekker, I.; Zhang, B.; Hendi, A.H.; Ahmad, A.; Ahmad, S.; Zada, N.; Ahmad, H.; Shah, L.A.; et al. Review on Methylene Blue: Its Properties, Uses, Toxicity and Photodegradation. *Water* **2022**, *14*, 242. [CrossRef]
71. Mittal, A.; Malviya, A.; Kaur, D.; Mittal, J.; Kurup, L. Studies on the adsorption kinetics and isotherms for the removal and recovery of methyl orange from wastewaters using waste materials. *J. Hazard. Mater.* **2007**, *148*, 229–240. [CrossRef]
72. Guilherme, M.R.; Silva, R.; Girotto, E.M.; Rubira, A.F.; Muniz, E.C. Hydrogels based on PAAm network with PNIPAAm included: Hydrophilic–hydrophobic transition measured by the partition of Orange II and Methylene Blue in water. *Polymer* **2003**, *44*, 4213–4219. [CrossRef]
73. Cho, H.; Zoh, K.-D. Photocatalytic degradation of azo dye (Reactive Red 120) inTiO_2/UV system: Optimization and modeling using a responsesurface methodology (RSM) based on the central composite design. *Dyes Pigment.* **2007**, *75*, 533–543. [CrossRef]
74. Birke, V.; Schuett, C.; Burmeier, H.; Friedrich, H.-J. Impact of trace elements and impurities in technical zero-valent iron brands on reductive dechlorination of chlorinated ethenes in groundwater. In *Permeable Reactive Barrier Sustainable Groundwater Remediation*; Naidu, R., Birke, V., Eds.; CRC Press: Boca Raton, FL, USA, 2015; pp. 87–98, ISBN 978-1-4822-2447-4.
75. Phukan, M. Characterizing the Fe^0/sand system by the extent of dye discoloration. *Freib. Online Geosci.* **2015**, *40*, 1–70.
76. Phukan, M.; Noubactep, C.; Licha, T. Characterizing the ion-selective nature of Fe^0-based filters using azo dyes. *Chem. Eng. J.* **2015**, *259*, 481–491. [CrossRef]
77. Cao, V.; Alyoussef, G.; Gatcha-Bandjun, N.; Gwenzi, W.; Noubactep, C. Characterizing the impact of MnO_2 addition on the efficiency of Fe^0/H_2O systems. *Sci. Rep.* **2021**, *11*, 9814. [CrossRef] [PubMed]
78. Parks, G.A. The isoelectric points of solid oxides, solid hydroxides, and aqueous hydroxo complex systems. *Chem. Rev.* **1965**, *65*, 177–198. [CrossRef]
79. Kosmulski, M. Isoelectric points and points of zero charge of metal (hydr)oxides: 50 years after Parks' review. *Adv. Colloid Interface Sci.* **2016**, *238*, 1–61. [CrossRef]
80. Gatcha-Bandjun, N.; Noubactep, C.; Loura Mbenguela, B. Mitigation of contamination in effluents by metallic iron: The role of iron corrosion products. *Environ. Technol. Innov.* **2017**, *8*, 71–83. [CrossRef]
81. Burghardt, D.; Kassahun, A. Development of a reactive zone technology for simultaneous in situ immobilisation of radium and uranium. *Environ. Geol.* **2005**, *49*, 314–320. [CrossRef]
82. Moraci, N.; Calabrò, P.S. Heavy metals removal and hydraulic performance in zero-valent iron/pumice permeable reactive barriers. *J. Environ. Manag.* **2010**, *91*, 2336–2341. [CrossRef]
83. Btatkeu, K.B.D.; Miyajima, K.; Noubactep, C.; Caré, S. Testing the suitability of metallic iron for environmental remediation: Discoloration of methylene blue in column studies. *Chem. Eng. J.* **2013**, *215–216*, 959–968. [CrossRef]
84. Aragaw, T.A.; Alene, A.N. A comparative study of acidic, basic, and reactive dyes adsorption from aqueous solution onto kaolin adsorbent: Effect of operating parameters, isotherms, kinetics, and thermodynamics. *Emerg. Contam.* **2022**, *8*, 59–74. [CrossRef]
85. Miehr, R.; Tratnyek, G.P.; Bandstra, Z.J.; Scherer, M.M.; Alowitz, J.M.; Bylaska, J.E. Diversity of contaminant reduction reactions by zerovalent iron: Role of the reductate. *Environ. Sci. Technol.* **2004**, *38*, 139–147. [CrossRef] [PubMed]
86. Li, J.; Dou, X.; Qin, H.; Sun, Y.; Yin, D.; Guan, X. Characterization methods of zerovalent iron for water treatment and remediation. *Water Res.* **2019**, *148*, 70–85. [CrossRef] [PubMed]
87. Tepong-Tsindé, R.; Ndé-Tchoupé, A.I.; Noubactep, C.; Nassi, A.; Ruppert, H. Characterizing a newly designed steel-wool-based household filter for safe drinking water provision: Hydraulic conductivity and efficiency for pathogen removal. *Processes* **2019**, *7*, 966. [CrossRef]
88. Tepong-Tsindé, R. Designing and Piloting a household filter for the peri-urban population of Douala (Cameroon). *Freib. Online Geosci.* **2021**, *61*, 1–80.
89. Ndé-Tchoupé, A.I.; Konadu-Amoah, B.; Gatcha-Bandjun, N.; Hu, R.; Gwenzi, W.; Noubactep, C. Kanchan arsenic filters for household water treatment: Unsuitable or unsustainable? *Water* **2022**, *14*, 2318. [CrossRef]
90. Mueller, B.; Chan, M.C.K.; Hug, S.J. Unique geochemistry of arsenic-contaminated groundwater and corresponding mitigation efforts in Southern Nepal. *ACS ES&T Water* **2023**, *3*, 1527–1535. [CrossRef]
91. Lufingo, M.; Ndé-Tchoupé, A.I.; Hu, R.; Njau, K.N.; Noubactep, C. A novel and facile method to characterize the suitability of metallic iron for water treatment. *Water* **2019**, *11*, 2465. [CrossRef]
92. Naseri, E.; Ndé-Tchoupé, A.I.; Mwakabona, H.T.; Nanseu-Njiki, C.P.; Noubactep, C.; Njau, K.N.; Wydra, K.D. Making Fe^0-based filters a universal solution for safe drinking water provision. *Sustainability* **2017**, *9*, 1224. [CrossRef]
93. Hernandez, R.; Zappi, M.; Kuo, C.H. Chloride effect on TNT degradation by zerovalent iron or zinc during water treatment. *Environ. Sci. Technol.* **2004**, *38*, 5157–5163. [CrossRef]
94. Zhang, Y.; Wang, J.; Amrhein, C.; Frankenberger, W.T., Jr. Removal of selenate from water by zerovalent iron. *J. Environ. Qual.* **2005**, *34*, 487–495. [CrossRef] [PubMed]

95. Ansaf, K.V.K.; Ambika, S.; Nambi, I.M. Performance enhancement of zero valent iron based systems using depassivators: Optimization and kinetic mechanisms. *Water Res.* **2016**, *102*, 436–444. [CrossRef]
96. Gillham, R.W.; O'Hannesin, S.F. Enhanced degradation of halogenated aliphatics by zero-valent iron. *Ground Water* **1994**, *32*, 958–967. [CrossRef]
97. Lipczynska-Kochany, E.; Harms, S.; Milburn, R.; Sprah, G.; Nadarajah, N. Degradation of carbon tetrachloride in the presence of iron and sulphur containing compounds. *Chemosphere* **1994**, *29*, 1477–1489. [CrossRef] [PubMed]
98. Schreier, C.G.; Reinhard, M. Transformation of chlorinated organic compounds by iron and manganese powders in buffered water and in landfill leachate. *Chemosphere* **1994**, *29*, 1743–1753. [CrossRef]
99. Fu, F.; Dionysiou, D.D.; Liu, H. The use of zero-valent iron for groundwater remediation and wastewater treatment: A review. *J. Hazard. Mater.* **2014**, *267*, 194–205. [CrossRef]
100. Obiri-Nyarko, F.; Grajales-Mesa, S.J.; Malina, G. An overview of permeable reactive barriers for in situ sustainable groundwater remediation. *Chemosphere* **2014**, *111*, 243–259. [CrossRef]
101. Comba, S.; Sethi, R. Stabilization of highly concentrated suspensions of iron nanoparticles using shear-thinning gels of xanthan gum. *Water Res.* **2009**, *43*, 3717–3726. [CrossRef]
102. Ghauch, A.; Tuqan, A.; Assi, H.A. Antibiotic removal from water: Elimination of amoxicillin and ampicillin by microscale and nanoscale iron particles. *Environ. Pollut.* **2009**, *157*, 1626–1635. [CrossRef]
103. Perey, J.R.; Chiu, P.C.; Huang, C.-P.; Cha, D.K. Zero-valent iron pretreatment for enhancing the biodegradability of azo dyes. *Water Environ. Res.* **2002**, *74*, 221–225. [CrossRef]
104. Oh, S.Y.; Chiu, P.C.; Kim, B.J.; Cha, D.K. Zero-valent iron pretreatment for enhancing the biodegradability of RDX. *Water Res.* **2005**, *39*, 5027–5032. [CrossRef] [PubMed]
105. Sleiman, N.; Deluchat, V.; Wazne, M.; Mallet, M.; Courtin-Nomade, A.; Kazpard, V.; Baudu, M. Phosphate removal from aqueous solutions using zero valent iron (ZVI): Influence of solution composition and ZVI aging. *Colloids Surf. A Physicochem. Eng. Asp.* **2017**, *514*, 1–10. [CrossRef]
106. Cui, J.; Wang, X.; Zheng, K.; Wang, D.; Zhu, H.; Mao, X. Concentration-dependent enhancing effect of dissolved silicate on the oxidative degradation of sulfamethazine by zero-valent iron under aerobic conditions. *Environ. Sci. Technol.* **2019**, *54*, 1242–1249. [CrossRef] [PubMed]
107. Zubair, Y.O.; Fuchida, S.; Tokoro, C. Adsorption and microscopic analysis of arsenate uptake by mesoporous zerovalent iron–magnetite nanocomposite: A detailed study on coexisting ions effects. *Water Air Soil Pollut.* **2022**, *233*, 484. [CrossRef]
108. Noubactep, C. Characterizing the effects of shaking intensity on the kinetics of metallic iron dissolution in EDTA. *J. Hazard. Mater.* **2009**, *170*, 1149–1155. [CrossRef] [PubMed]
109. Noubactep, C.; Licha, T.; Scott, T.B.; Fall, M.; Sauter, M. Exploring the influence of operational parameters on the reactivity of elemental iron materials. *J. Hazard. Mater.* **2009**, *172*, 943–951. [CrossRef]
110. Alyoussef, G. Characterizing the Impact of Contact Time in Investigating Processes in Fe^0/H_2O Systems. Master's Thesis, University of Göttingen, Göttingen, Germany, 2019.
111. He, Y.; Guo, Z.; Chen, M.; Wan, S.; Peng, N.; Fu, X.; Yuan, D.; Na, B. Efficient adsorption of methyl orange and methylene blue dyes by a novel carbazole-based hyper-crosslinked porous polymer. *J. Porous Mater.* **2023**. [CrossRef]
112. Konadu-Amoah, B. Decontamination in Fe^0-Based Systems: Understanding Phosphate Removal in Fe^0/H_2O System Using the MB Method. Ph.D. Thesis, Hohai University, Najing, China, 2023.
113. Scott, T.B.; Popescu, I.C.; Crane, R.A.; Noubactep, C. Nano-scale metallic iron for the treatment of solutions containing multiple inorganic contaminants. *J. Hazard. Mater.* **2011**, *186*, 280–287. [CrossRef]
114. Zhang, Y.-F.; Zhang, C.-H.; Xu, J.-H.; Li, L.; Li, D.; Wu, Q.; Ma, L.-M. Strategies to enhance the reactivity of zero-valent iron for environmental remediation: A review. *J. Environ. Manag.* **2022**, *317*, 115381. [CrossRef]

Disclaimer/Publisher's Note: The statements, opinions and data contained in all publications are solely those of the individual author(s) and contributor(s) and not of MDPI and/or the editor(s). MDPI and/or the editor(s) disclaim responsibility for any injury to people or property resulting from any ideas, methods, instructions or products referred to in the content.